PIV Study on Flow Fields of Spray and Surrounding Gas under Non-Evaporating and Evaporating Conditions

J. Y. Zhu*, K. Nishida and O. A. Kuti
Department of Mechanical System Engineering, University of Hiroshima, Japan
zhujingyu-scl@hiroshima-u.ac.jp, nishida@mec.hiroshima-u.ac.jp, kuti@hiroshima-u.ac.jp

Abstract

The measurements of spray induced surrounding gas motion and spray flow were carried out by using LIF-PIV (Laser Induced Fluorescence-Particle Image Velocimetry) and PIV technique, respectively. The behaviors such as spray flow and gas flow velocity distributions, the ambient gas mass flow rate into the spray were compared quantitatively in both non-evaporating and evaporating conditions. Two injection pressures (100, 300MPa) and a micro-hole nozzle with diameter of 0.08mm were used. The results show the significant difference in the gas flow characteristics between non-evaporating and evaporating conditions. The total ambient gas flow mass is restricted in the evaporating condition. By comparing the droplets flow in the non-evaporating spray and the vapor phase flow in the evaporating spray, even though there is no much difference of the mean velocity distribution, the stronger vortex motion and faster spray momentum depletion can be observed in the evaporating condition, which results in a more homogeneous fuel/gas mixture and restricted penetration length. Higher injection pressure enhances the mean flow velocity and the small scale vortex distribution in the whole region, which implies the promotion of the fuel/gas mixing process. The vorticity distribution inside the spray corresponds to the resultant heterogeneity of the fuel concentration distribution. The fuel parcel with different mass concentration determines flow velocity distribution and the spray development.

Introduction

The spray/surrounding gas mixing process exerts a great influence on the mixture formation and subsequent combustion behavior in D.I. Diesel engines, thus it deserves more insightful understanding. So far there have been very few published works concerning the surrounding gas flow of the diesel spray. Rhim et al.[1, 2] systematically investigated the surrounding gas flow of the non-evaporating, evaporating and burning spray along the side surface and concluded that entrained gas velocity is larger and the entrained gas mass at the spray tip is expected to reduce for the evaporating spray condition. Yeom. [3] also investigated the effect of the injection pressure on the mixture formation of the evaporating diesel spray by using PIV technique. As for the spray flow, some studies [4, 5] successfully measured the internal velocity distribution of the non-evaporating spray by capturing the image of diluted spray droplets or the fluorescent tracers dissolved in the fuel.

This study attempts to quantitatively investigate the gas flow velocity and mass flow characteristics at the side periphery and the tip periphery of both the non-evaporating and evaporating spray with high injection pressure. Secondly, the spray internal flow, especially the vapor phase flow of the diesel spray was measured. At last, the characteristics of ambient gas flow and spray internal flow were considered comprehensively. The results of this work extend the understanding of the spray formation process, which is also available for the validation of the CFD result.

Experimental Methods

The PIV measurement of the ambient gas flow was carried out in a constant volume chamber to achieve the quiescent ambient condition. The sufficient chamber's volume ensures that the free spray develops in the nearly quiescent condition. Three quartz windows with a diameter of 100mm were installed at the three sides of chamber respectively. A kanthal alloy heating unit was placed on the bottom of the chamber to produce the high temperature atmosphere as high as 1000K. Two thermal couple antennas were inserted to detect the ambient temperature in different position without the intrusion to the spray.

In the case of non-evaporating spray, the water solution of Rhodamine B reagent as the fluorescent tracing particle was injected into high pressure chamber from one side by a swirl type injector with an injection pressure of 9MPa. The tracer droplets' size distribution impacts the tracking ability with the gas flow, according to the measurement result in the previous work [6], the overall AMD value was restricted lower than 6μm by adjusting the interval between the tracer injection and the Diesel fuel injection. At the desired measuring timing after Diesel fuel injection, an Nd:YAG laser sheet with a wavelength of 532nm and thickness of 1mm was incident from

* Corresponding author: zhujingyu-scl@hiroshima-u.ac.jp

the opposite side of the vessel and traversed through the spray axis, the tracing particles emitted the fluorescent light with the wavelength of more than 590nm. Meanwhile the CCD camera which was mounted with the long pass filter (>560nm) and placed at the position perpendicular to the laser sheet was synchronized to capture two images with high spatial resolution of 1600×1200 pixels during a short time interval. The scattering signal of the spray droplets was cut off and only the fluorescent light from the tracer particles was recorded. The two-dimensional ambient gas flow field was calculated based on the displacement of tracers recorded in the double frames according to the cross correlation algorithm.

In the case of the evaporating spray, the MgO solid powder with the size of 2μm substitutes the water solution of Rhodamine B as the tracer. Since very few fluorescent matters are available in the visible laser light range in the high temperature condition, the Mie scattering light from the MgO powder was directly recorded by the PIV system and used for analyzing. Unlike the LIF-PIV measurement for the non-evaporating spray in which the gas flow very closed to the spray boundary could also be obtained, the gas flow analysis for the evaporating spray starts from a certain distance away from the spray periphery due to the influence of the strong light scattered from the liquid core region and the existence of the vapor phase.

As for the measurement of the spray internal flow, a localized photography of the spray droplets particularly focusing on the downstream region of the spray was applied in the non-evaporating case. The time interval between the double frames and the size of the interrogation window need to be carefully adjusted compared with that of the ambient gas flow measurement due to the significant difference of the velocity scale. The spray droplets themselves were treated as the tracer to calculate the spray droplets movement.

Due to the unclear physical properties especially the boiling point of the diesel fuel, the mixture of dodecane and silicon oil was selected as the surrogate fuel in measuring the vapor phase flow of the evaporating spray. Firstly, the pure dodecane reagent was injected into the prescribed high temperature and high pressure atmosphere to determine the liquid length and the complete vaporization location. In the formal experiment, 95%/vol. of the dodecane was mixed with 5%/vol. of the silicon oil which has remarkable higher boiling point, thus It is proper to consider that the remaining droplets downstream of the complete vaporization location are composed of the silicon oil. Kosaka et al. [7] concluded that the silicon droplets follow the turbulent flow of the vapor phase, and the multiple scattering of the silicon droplets can be negligible. Several options of the proportion of the silicon oil were tested and 5% was selected at last according to the scattering light intensity and distributing number density of the silicon droplets and the physical property of the mixing fuel.

In order to eliminate the shot-by-shot variation in measuring the ambient gas flow field, the results from several samples (at least 6 shots) with good repeatability were averaged and used for analysis. On the other hand, the averaging of the spray internal flow result might lose the detailed velocity fluctuation information which varies in the different shots, thus the results of several single shots are shown together in this work.

Table 1 summarizes the experiment conditions in this work.

Table 1 Experimental Conditions

Nozzle Diameter (mm)	0.08			
Injection Pressure (MPa)	100, 300			
Injection Duration (ms)	2.2			
Ambient Gas	Nitrogen			
Ambient Gas Density (kg/m^3)	15			
Measurement	Ambient Gas Flow		Spray Internal Flow	
Ambient Condition	Non-Evaporating	Evaporating	Non-Evaporating	Evaporating
Ambient Temperature (K)	300	770	300	770
Ambient Pressure (MPa)	1.4	3.5	1.4	3.5
Test Fuel	Diesel JIS#2	Diesel JIS#2	Diesel JIS#2	5%/vol. Silicon Oil (KF-95-50cs) + 95%/vol. Dodecane
Fuel Density (kg/m^3)	~860	~860	~860	760
Kinematic Viscosity (mm^2/s)	5-6	5-6	5-6	4.2
Boiling Point (K, 1bar)	450~630	450~630	450~630	~520
Measuring Method	LIF-PIV	PIV	PIV	PIV
Interrogation Window	16*16 pixels (1.55mm*1.55mm)	16*16 pixels (1.55mm*1.55mm)	16*16 pixels (0.94mm*0.94mm)	16*16 pixels (0.94mm*0.94mm)
Frame Interval (μs)	40	40	5	5

Results and Discussion

1. Ambient Gas Flow Measurement

Figure 1 shows the comparison of the spatial distribution of the ambient gas flow velocity at several timings after SOI in both (a) non-evaporating and (b) evaporating conditions. Rather than the diluted spray droplets interact with the ambient gas in the non-evaporating condition, the liquid core region keeps almost constant after reaching the quasi-steady state in the evaporating condition, the vapor phase downstream pushes the ambient gas out. As described in the previous work [6], the the spatial distribution of spray-ambient gas interaction is categorized as three regions: (1) Entrainment section at the side periphery. Here the ambient gas is entrained into the spray periphery because of the pressure gradient from the surrounding air to the spray induced by fuel injection. The side periphery in this section is quite smooth and almost stable. (2) Capturing section at the spray tip periphery. The spray droplets at the spray tip region move downstream with sufficient momentum. A large amount of ambient gas is captured into the spray plume due to the substantial relative velocity of spray penetration and ambient gas motion. (3) Recirculation section downstream of the side periphery. In this section, the droplets at the spray tip gradually lose momentum and are pushed aside by the upstream droplets and ambient gas flow, resulting in the simultaneous movement of droplets and ambient gas in the radial direction. At the same time, due to the influence of the relatively lower pressure of the ambient gas outside of the entrainment section, the droplets and ambient gas flow towards the upstream direction.

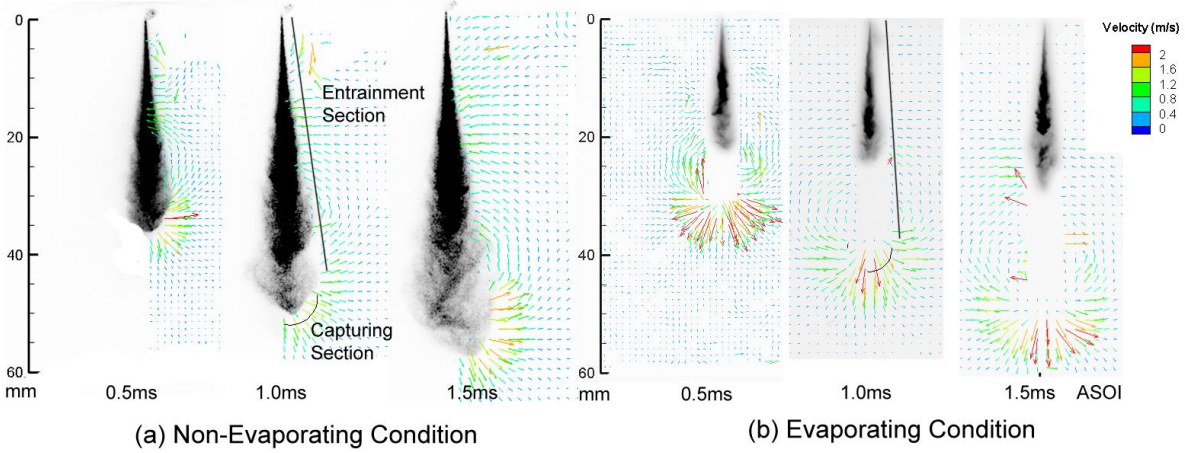

Figure 1 Spatial Distribution of Ambient Gas Flow Velocity (Pinj=100MPa)

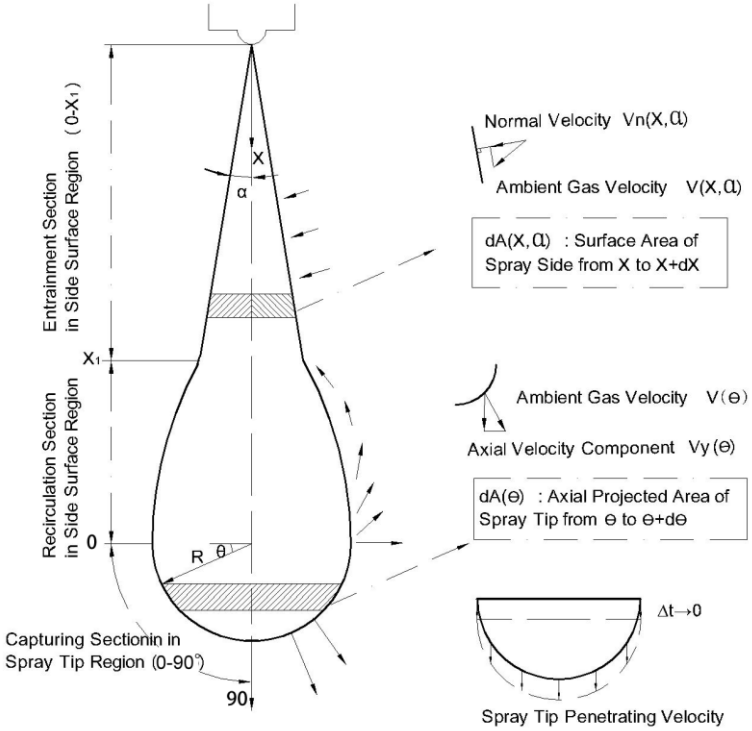

Figure 2 Calculating Model for Ambient Gas Mass Flow

Figure 2 summarizes the categorization of the ambient gas flow sections, this model also defines the method of the measurement of the gas flow velocity and the calculation of the mass flow rate as shown below. Figure 3

shows the comparison of the normal velocity along the side surface at the entrainment section. It is worth emphasizing that the gas flow analysis for the evaporating spray starts from a certain distance away from the spray periphery, correspondingly, the control surface for the non-evaporating spray is also drawn with the same distance. Because of the square profile of the fuel injection rate, the maximum gas velocity keeps constant after reaching the quasi-steady state, while the entrainment section length increases with the time. The gas velocity for the non-evaporating case shows a slight larger value than that of the evaporating case. In contrast, Rhim, D. R. et al. [1] argued that the normal velocity for the evaporating case might increase by 0.5m/s due to the enhanced temperature gradient from the outside to the evaporating liquid region and the enhanced gas viscosity. On the other hand, the factors such as the reduced aerodynamic force on the spray/gas interface due to the relatively lower spray flow velocity, and the outward expansion of vapor phase tend to decrease the entrained gas flow velocity.

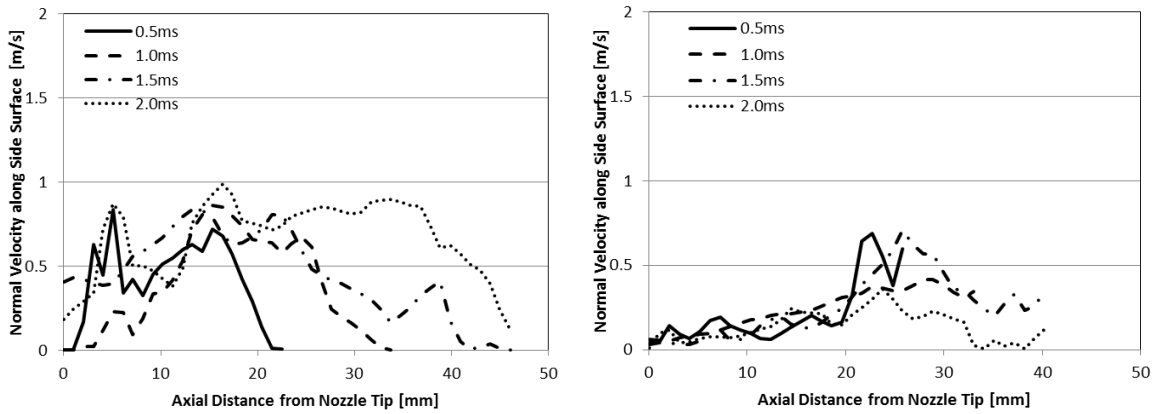

(a) Non-Evaporating Condition (b) Evaporating Condition

Figure 3 Comparison of Normal Velocity Distribution along Side Surface

The dominant factor lies in the tip region. Providing that the spray tip region is assumed to be a regular half sphere, the distribution of the axial component of the pushed out gas flow velocity along the quarter circle (90 deg. stands for the spray tip) at the capturing section is shown in Fig.4. Since it is difficult to determine the vapor phase boundary by using the current data, the location where the maximum velocity appears is assumed to be spray boundary. In contrast, the spray tip penetrating velocity at each timing is also denoted in the figure. A considerable increase of the pushed out gas velocity can be found in the evaporating case, in contrast, the spray penetrating velocity for the evaporating case decreases due to the faster momentum loss of the vapour phase. The increased gas flow velocity is attributed to the partial pressure taken by the fuel vapour, which restricts the amount of gas inside the spray plume, if the ambient density keeps the same. In the non-evaporating case, the whole spray volume consists of the ambient gas because the fuel vaporization is negligible. As an extreme condition, the much smaller velocity difference between the jet displacement and the ambient gas can be observed in the pure gas jet condition, which was reported in the work in the reference [8]. The local fuel vapor/gas pressure is considered to determine the amount the ambient gas flow.

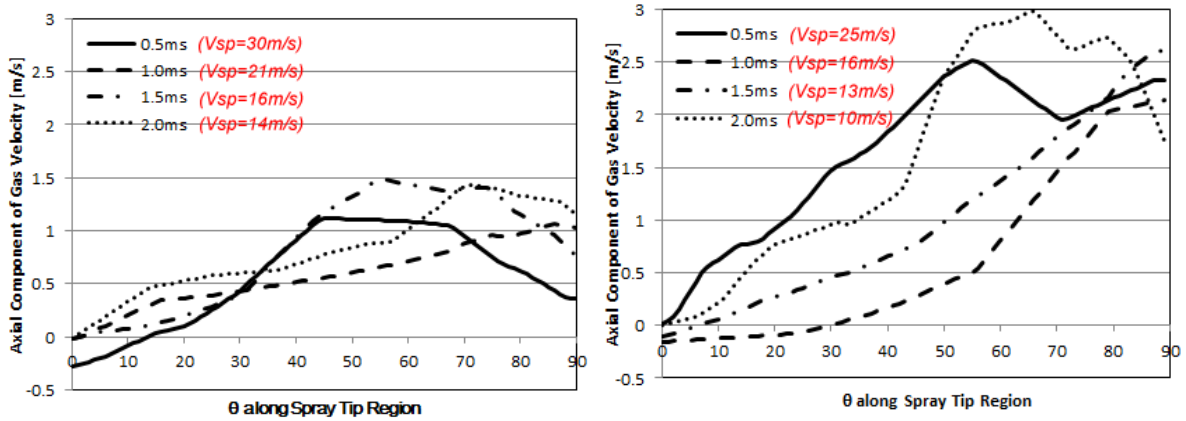

(a) Non-Evaporating Condition (b) Evaporating Condition

Figure 4 Comparison of Axial Velocity Component Distribution along Spray Tip Region

According to the model proposed in the previous work [6], the total gas mass flow rate result is shown in Fig.5, in which the $\dot{M}_{a(ent)}$ indicates the gas flow at the entrainment section, while the $\dot{M}_{a(cap)}$ indicates the

gas flow at the capturing section. The curve shows the instantaneous ratio of gas/fuel mass flow rate. In both the non-evaporating and evaporating cases, a large proportion of the ambient gas flow is taken from the capturing section. Rhim et al. [1] presented the similar results by comparing with the spray volume. However, because of the significant reduction of gas flow at the tip region, the proportion of the gas flow at the entrainment region in evaporating case rises to 10%-21%, compared with 8%-18% in non-evaporating case, which implies that the gas flow along the side periphery plays a more important role in the evaporating spray condition. The gas flow in the tip periphery would be further restricted due to the heat release effect [9]. The total ambient gas flow and the instantaneous Ma/Mf for the evaporating case decreases remarkably especially in the later stage of the fuel injection, since the vapor phase at the spray tip loses the momentum faster.

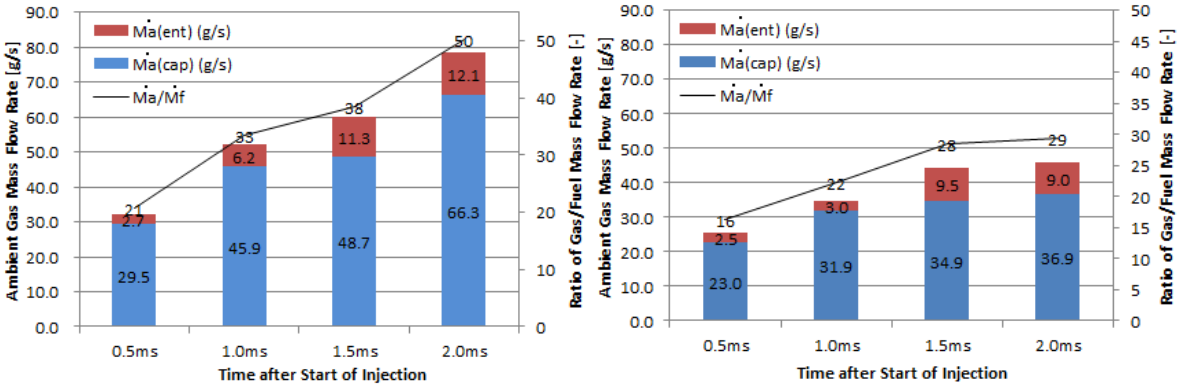

(a) Non-Evaporating Condition (b) Evaporating Condition

Figure 5 Comparison of Gas Mass Flow Rate Result

2. Spray Internal Flow Measurement

Figure 6 shows several samples of the flow field of the spray droplets with the injection pressure of 100MPa under the non-evaporating condition. Only the downstream part of the spray is magnified and analysed to avoid the impact of the strong scattering light from the upstream part. The Mie scattering spray images of the corresponding samples are also shown together to take into account of the result of fuel mass concentration distribution, because the Mie scattering light intensity is related to the number and size of local droplets. The maximum velocity usually locates along the centreline of the spray, while attenuates gradually with the radial direction. In particular, the droplets near the spray periphery downstream tends to be pushed aside and move upward, which corresponds to the recirculation region observed in the ambient gas flow measurement, as a result the large scale vortex motion forms. The intermittent distribution of the droplets velocity can be found in all the samples, which is owing to the turbulent fluctuation in the flow field, the numerical simulation result with LES turbulent model is capable to show the similar flow field characteristics [10]. It is believed that the spray penetration is based on such process: the spray droplets parcel injected in advance losses the momentum, then is surpassed and pushed aside by the successive parcel with higher velocity. This process results in the incoherent velocity distribution and mass concentration distribution. Due to the ambient gas resistance, the spray droplets movement usually bifurcates in the tip region, rather than moving straightforward. The magnified A region in Fig.7 highlights such behaviour, it can be also observed in region A that the parcel with larger droplet size or more fuel mass has more momentum to develop further downstream. Such kind of parcels at the tip region determines the whole spray development. On the other hand, the vortex like motion appears on both sides of the main flow path, the lower fuel mass concentration can be found in the centre of the vortex structure due to the centrifugal force impact.

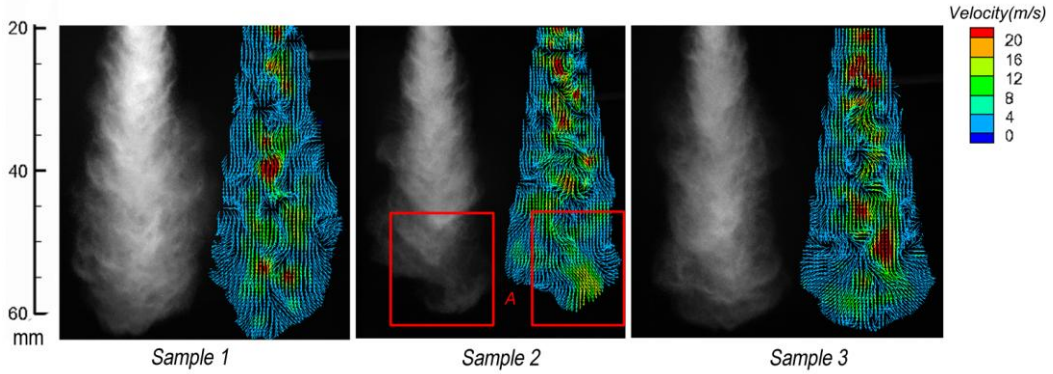

Figure 6 Flow Field of Spray Droplets in Non-Evaporating Condition (Pinj=100MPa, 2.0ms ASOI)

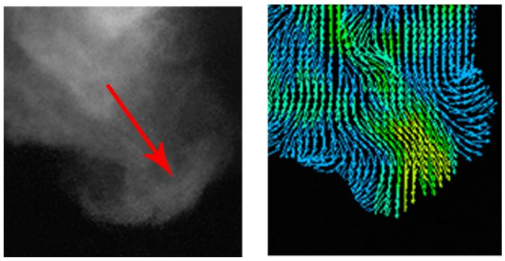

Figure 7 Magnified Region A Shown in Figure 6

The effect of the fuel injection pressure on the droplets movement is shown in Fig.8. It is evident that the mean value of the droplets velocity increases with the fuel injection pressure especially at the spray tip region, which leads to the longer penetration length. The small scale vortex motion, in other word, the spatial variation of the velocity distribution becomes more significant in the whole region, which implies that the small scale turbulent mixing can be effectively enhanced with the increase of fuel injection pressure, as a result, the fuel/gas mixing process is promoted.

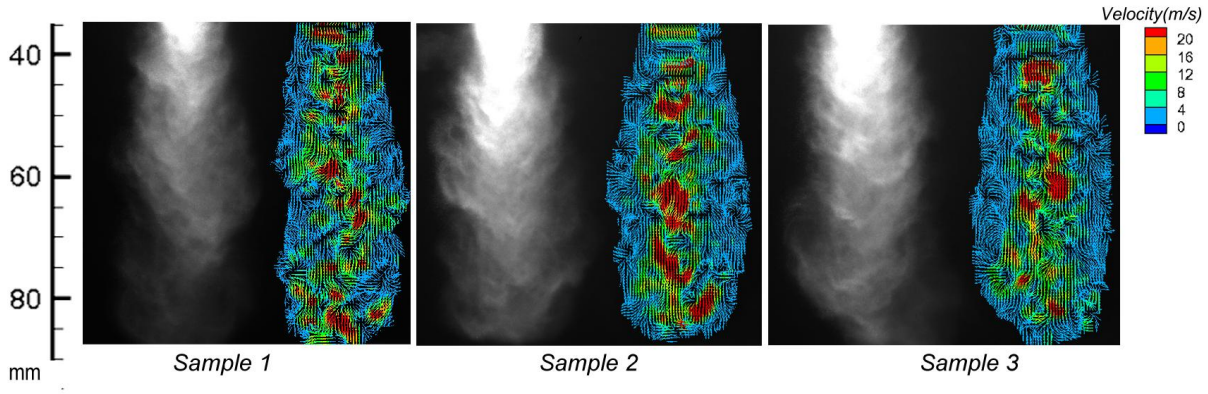

Figure 8 Flow Field of Spray Droplets in Non-Evaporating Condition (Pinj=300MPa, 2.0ms ASOI)

Several samples of the vapor phase flow field under the evaporating condition coupled with the Mie scattering signal image of the silicon droplets are shown in Fig.9. The ambient density was kept constant as that in the non-evaporating conditions. Compared with the non-evaporating spray, the evaporating spray periphery fluctuates remarkably with different shots, which also corresponds to the shot-by-shot variation of the flow field. Especially at the spray tip region, unlike the flow field shown in Fig.6, the irregular vapor phase even flows towards the radial direction. This is because that the vapor phase with less momentum is subjected to the resistance of the surrounding gas at the tip region much easier. Even though the spray flow velocity shows the similar value as the non-evaporating condition upstream, as a result, the evaporating spray penetrates shorter than non-evaporating spray under the same ambient gas density condition.

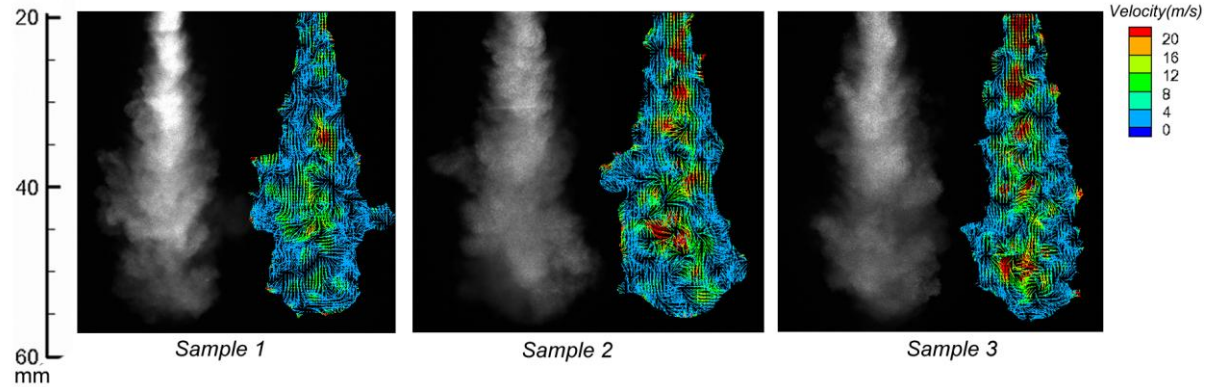

Figure 9 Flow Field of Spray Vapor Phase in Evaporating Condition (Pinj=100MPa, 2.0ms ASOI)

By selecting three samples from Fig.6-9, the vorticity distribution of the flow field was calculated according to the following equation (1):

$$w_{ij} = \frac{du_{ij}}{dy_{ij}} - \frac{dv_{ij}}{dx_{ij}} \quad (1)$$

In which the u, v stand for radial and axial component of the flow velocity respectively, the x, y are the co-ordinate of the flow field. The results are shown in Fig.10. It is notable that the vortex intensity enhances with the increase of the fuel injection pressure or the increase of the ambient temperature. Particularly, the significant vortex distribution extends to the tip region in evaporating condition, which has the tendency to improve the fuel/gas mixing process. Several dynamic and thermodynamic reasons can be considered such as the increased gas viscosity, the strong gas density gradient and the heat transfer. The magnified region A, B shown in Fig. 11 indicates that larger fuel mass concentration usually locates along the streamline of the vortex motion, the lower fuel mass concentration can be found in the centre of the vortex structure due to the centrifugal force effect. As a conclusion, the vorticity distribution corresponds to the resultant heterogeneity of the fuel concentration distribution.

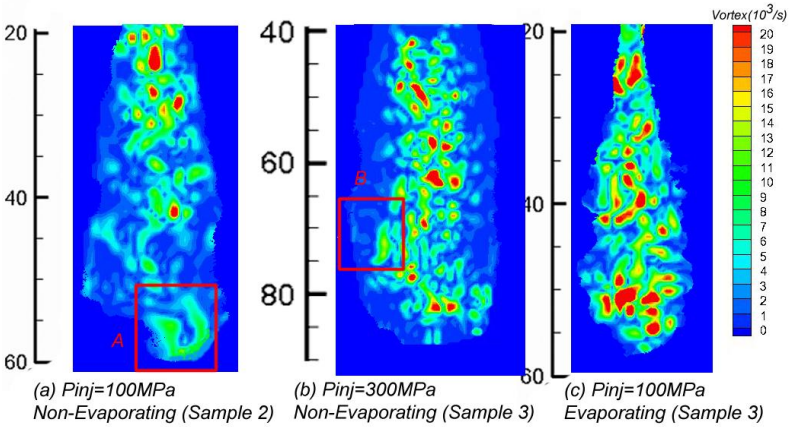

Figure 10 Vorticity Distribution of Flow Field (2.0ms ASOI)

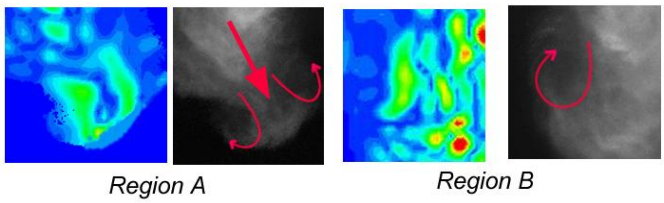

Figure 11 Magnified Region A and B Shown in Figure 9

Figure 12 and 13 statistically analyse the probability distribution function of the flow velocity value and the vortex intensity value of the three samples used in Fig.10 respectively. It is found that with the increase of the fuel injection, the spray flow velocity and vorticity intensity with larger value take up a larger proportion. It is worth noticing that under the evaporating condition, the mean flow velocity is apparently larger than that in non-evaporating condition, even approaches to the value with the injection pressure of 300MPa. However, due to the strong turbulent mixing and flow fluctuation inside the spray, the tip penetration inversely decreases. This can be proved in Fig. 13, in which the evaporating spray shows the highest value of mean vorticity.

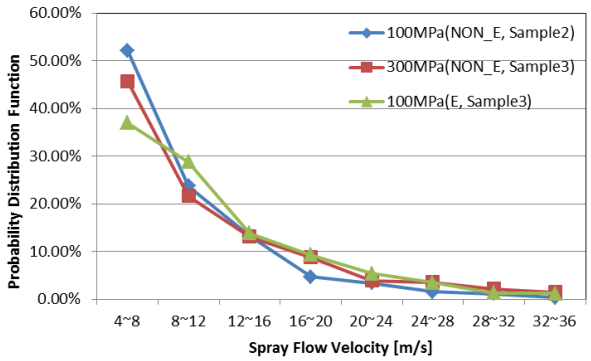

Figure 12 Probability Distribution Function of Spray Flow Velocity

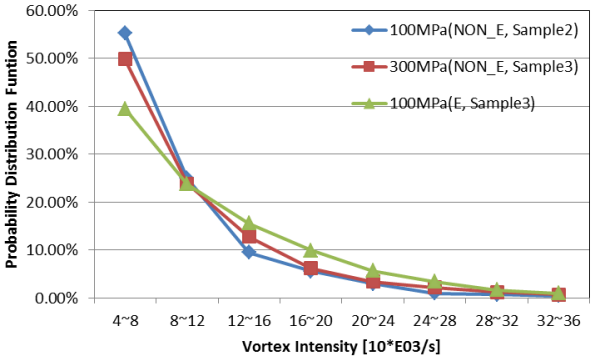

Figure 13 Probability Distribution Function of Vortex Intensity

3. Discussion

It is worth clarifying the phenomenon the ambient gas flow distribution under the non-evaporating spray, evaporating spray and ultimately the gas jet especially at the tip region, and relating to the spray internal flow characteristics. The LIF-PIV and PIV measurement result shown in this work indicates that large amount of ambient gas flow is attributed to the flow at the tip region regardless of the non-evaporating or evaporating condition. However, the detailed proportion changes according to the physical and thermodynamic condition. It is found that the spray droplets still move downwards smoothly in Fig.6, because the ambient gas can easily enters the interval among the discrete droplets, as a result, a large velocity difference between the spray tip penetration and the pushed-out gas was measured in Fig. 4. On the other hand, the strong velocity fluctuation shown in Fig.9 indicates that the vapor phase at the tip region is subjected to the strong resistance from the outside gas, as shown in Fig.4, the ambient gas is pushed aside with higher velocity under the evaporating condition. The exact gas flow velocity and gas mass flow rate at the tip region depend on the local fuel vapor pressure, the vapor flow velocity and the vortex intensity.

Summary and Conclusions

The measurements of spray induced surrounding gas motion and spray flow were carried out using LIF-PIV (Laser Induced Fluorescence-Particle Image Velocimetry) and PIV technique, respectively. The behaviors such as spray flow and gas flow velocity distribution, the ambient gas mass flow rate into the spray were compared quantitatively under both non-evaporating and evaporating conditions. Several conclusions are summarized and presented as follows:

1. For the ambient gas flow measurement, the gas velocity along the side surface for the non-evaporating case shows a slight larger value than that of the evaporating case. On the other hand, a considerable increase of the pushed out gas velocity at the tip region can be found in the evaporating case, in contrast, the spray penetrating velocity for the evaporating case decreases due to the faster momentum loss of the vapor phase.

2. A large amount of ambient gas flow mass is attributed to the flow at the tip region regardless of the non-evaporating or evaporating condition. However, the detailed proportion changes according to the physical and thermodynamic condition. The role of the gas flow along the side periphery becomes more important in evaporating spray condition.

3. For the spray internal flow measurement, the vorticity distribution inside the spray corresponds to the resultant heterogeneity of the fuel concentration distribution. Furthermore, the fuel parcel with different mass concentration also determines flow velocity distribution and the spray development.

4. Higher injection pressure enhances the mean flow velocity and the small scale vortex distribution in the whole region, which implies the promotion of the fuel/gas mixing process.

5. The much stronger vorticity and flow fluctuation inside the spray can be observed in the evaporating case, and the mean velocity value kept almost constant compared with that in non-evaporating case.

6. The ambient gas flow velocity and gas mass flow rate at the tip region depend on the local fuel vapor pressure, the vapor flow velocity and the vortex intensity.

In the future work, the comparison of the measurement result and the CFD simulation result will be carried out.

Acknowledgements

The authors would like to appreciate ISUZU advanced engineering center which provides high pressure injection system and the sponsor.

References

[1] Rhim, D. R., and Farrell, P. V., *SAE Paper* 2002-01-0499 (2002).
[2] Rhim, D. R., and Farrell, P. V., *SAE Paper* 2002-01-2668 (2002).
[3] Yeom, J., *Journal Mechanical Science and Technology* 22: 1785-1792 (2008).
[4] Cao, M., Nishino, K., Mizuno, S., and Torii, K., *Experiments in Fluid* 29: 211-219 (2000).
[5] Hillamo, H., Kaario, O., and Larmi, M., *SAE Paper* 2008-01-0942 (2008).
[6] Zhu, J.Y., Nishida, K., Kuti, O. A., and Moon, S., *Atomization and Sprays* 21-6: 447-465 (2011).
[7] Kosaka, H., Won, Y. H., and Kamimoto, T., *SAE Paper* 920107 (1992).
[8] Bruneaux, G., and Causse, M., *SAE Paper* 2011-01-1828 (2011).
[9] Han, D., Mungal, M. G., *Combustion and Flame*, 124: 370–386 (2001).
[10] Hori, T., Senda, J., Kuge, T., and Fujimoto, H., *SAE Paper* 2006-01-3334 (2006).